Available online at www.sciencedirect.com

jmr&t Journal of Materials Research and Technology

journal homepage: www.elsevier.com/locate/jmrt

Original Article

Utilization of waste slate powder in poly(lactic acid) based composite for 3D printer filament

Imtiyaz Khan [a], *Neeraj kumar* [a], *Jandel Singh Yadav* [b], *Mahavir Choudhary* [b], *Aditya Chauhan* [c], *Tej Singh* [d,*]

[a] *Mechanical Engineering Department, Suresh Gyan Vihar University, Jaipur-302017, India*
[b] *Mechanical Engineering Department, Srajan Institute of Technology, Management & Science, Ratlam-457001, India*
[c] *Department of Paper Technology, Indian Institute of Technology Roorkee-247667, India*
[d] *Savaria Institute of Technology, Faculty of Informatics, ELTE Eötvös Loránd University, Szombathely-9700, Hungary*

ARTICLE INFO

Article history:
Received 11 January 2023
Accepted 6 March 2023
Available online 8 March 2023

Keywords:
Fused deposition modelling
3D printing
Poly(lactic acid)
Slate powder

ABSTRACT

This work aims to develop and validate a novel composite material for fused deposition additive manufacturing utilizing poly (lactic acid) (PLA) and discarded slate powder. The slate powder is mixed into PLA filaments at varying percentages (0%, 5%, 10%, and 15%) using a twin screw extruder. The resulting filaments are used in a 3D printer to print the test specimens. The tensile strength of the testing specimens is improved up to 5 wt% by incorporating slate powder. In contrast, the tensile modulus, hardness, and impact strength are raised with slate powder up to 15 wt% in PLA-based filament by 19.03%, 10.67%, and 31.63%, respectively. The maximum flexural strength and modulus values are 93.25 MPa and 4.15 GPa, respectively, achieved at 10 wt% slate powder content PLA matrix. Moreover, slate powder's presence significantly affects the composites' dynamic mechanical properties, such as storage, loss modulus, and damping factor. The composite's entanglement density, C-factor, adhesion efficiency, and reinforcing efficiency factor are investigated using dynamic mechanical properties and correlated with their structural integrity. Results show that 10 wt% slate powder in the PLA matrix is sufficient for their successful application.

1. Introduction

Over the past few decades, the application of additive manufacturing technologies in medical, automotive, and aerospace fields has been exponentially growing due to higher accuracy and rapid manufacturing with less wastage of material [1,2]. Moreover, it enables the creation of specialized structural components with complex geometry that would be challenging or impossible to obtain using conventional methods. The additive manufacturing technology known as fused deposition modeling (FDM) is one of the most widely

* Corresponding author.
E-mail address: sht@inf.elte.hu (T. Singh).
https://doi.org/10.1016/j.jmrt.2023.03.046

used technologies for printing poly (lactic acid) (PLA), polycarbonate, polyamide, and a blend of the two thermoplastics with considerable design flexibility [3–5]. With the exhaustion of petroleum resources and their environmental aspect, a researcher currently focused on finding substitutes for products made of petroleum. PLA is a type of polymer that is environmentally friendly. It is made from lactic acid, which can be derived from plant sources such as corn and potato starch. It has distinctive qualities, such as being renewable, sustainable, biocompatible, and compostable [6–8]. PLA is a thermoplastic alternative that may be manufactured in the same manner as polyethylene, polypropylene, and other synthetic polymers, often by extrusion, thermoforming, blowing, and injection molding [6,9]. It makes films, sheets, bottles, and different kinds of thermoforms. PLA is the stiffer polymeric material, which is not very tough. The tensile elongation at breaking is generally less than 20% [10]. So, making PLA stronger is necessary if researchers want to use it for more things (e.g., agricultural products, packaging, etc.).

These polymers, however, generally need to gain more of owning technical or engineering polymers' typical properties. Nevertheless, these polymers do not reach, in general, specific properties of technical or engineering polymers. Including filler in polymer composite is responsible for boosting the composites' mechanical, thermal, and electrical properties [11]. For this reason, it is interesting for researchers to study the effect of PLA-based composite reinforced with various materials. Adding filler may also reduce the number of voids in the matrix, increasing the stiffness of the composite. The amount of fillers in a fiber-reinforced composite affects its mechanical properties because more filler encourages better particle-particle interaction and fiber-particle-matrix interaction, which may not be possible when fillers are present in optimal or suboptimal amounts [12,13]. Prashantha and Roger [14] investigated the mechanical performance of graphene-filled PLA filaments. Adding 10 wt% graphene to PLA increases the elastic modulus by 30% and the ultimate tensile strength by 27% while marginally decreasing the strain. Guo et al. [15] investigated the impact of adding thermoplastic polyurethane, polycaprolactone, and poly (ethylene-co-octene) together with various graft copolymer contents to poplar wood flour/PLA composites. The composites' impact strength, tensile strength, and flexural strength were all enhanced by 33.98%, 10.38%, and 51.31%, respectively, by adding thermoplastic polyurethane. This material proved more compatible with PLA composites made from wood flour than other toughening agents. At 5 wt% wood flour and 2 wt% graft copolymer, composite impact and tensile strength were increased by 7.75% and 8.39%, respectively.

Waste leather buff was employed as filler in the PLA by Ambone et al. [16], who also investigated the impact of the filler loading on the mechanical characteristics of the PLA composite. A peak in tensile strength and modulus was obtained for 10 wt% filler loading; then, it declined with more filler addition. Hamdan et al. [17] utilized rice husk powder in PLA composite and studied the performance at a different weight percentage of the rice husk in PLA composite. As the amount of filler in the PLA increased, it was observed that its tensile strength dropped. Increased rice husk powder was not related to a discernible rise in either the tensile modulus or the material's flexural strength. Nagarjun et al. [18] investigated the influence on PLA performance by adding filler as tamarind and date seed. The filler reinforcement significantly increased the PLA composite's strength and remained maximum for 3 wt % filler loading. An enhancement of 27.36%and 50.24% in tensile strength was noted for date and tamarind fillers. Clarizio and Tatara [19] observed the influence of incorporating glycerol-plasticized DDGS (distillers' dried grains with soluble) into the PLA matrix on its mechanical behavior. Adding glycerol-plasticized DDGS lowered the tensile strength of PLA, although the inclusion of 20–30 wt% filler decreased the strength by 60%. While 35 to 50 wt% filled PLA had approximately one-fifth the performance of pure PLA, and at higher filler loading (60–65 wt%), about 10% tensile strength remained. Koutsomitopoulou et al. [20] recycled the waste material from the olive oil mill and blended it with PLA to investigate its influence on the physical and mechanical properties. The poor interfacial bonding among olive pit powder and PLA may lead to a rise in tensile modulus but a decrease in flexural strength with reinforcement content.

Altun et al. [21] investigated the impact of Pistachio shell (10–30 wt%) loading in PLA-based composite. Tensile and flexural analyses revealed that combining 20% of the pre-treated Pistachio shell with PLA resulted in a composite with optimal mechanical characteristics. Yang et al. [22] developed a PLA/carbon nanotube (CNT) filament for the FDM technique. To investigate the workability of the PLA/CNT filament, the consequences of CNT content on the crystallization-melting mechanism and melt flow rate were examined. The analysis shows that the CNT proportion considerably impacted the mechanical and conductivity properties. Including 6 wt% CNT increased tensile strength by 64.12% and flexural strength by 29.29%. To improve the flame retardancy of PLA composites, Zhang et al. [23] proposed an innovative flame-retardant additive based on phosphate-mixed urea-grafted bamboo charcoal. A 3.8% reduction in tensile strength of PLA was reported for 10 wt% filler (grafted bamboo charcoal), while this loss increased to 14.5% for 30 wt% filler loading. The modulus of the PLA composites was reported to increase with grafted bamboo charcoal inclusion, indicating that the composites became more rigid and stiff.

Slate is a building material most commonly used for the roofing of buildings [24]. However, the extraction of helpful slate generates a massive amount of waste. It is reported in the literature that about 30 tons of waste powder are generated for one ton of slate product [25]. The use of this waste in producing valuable goods will not only be helpful from the point of view of ecology. But, it will also be beneficial from the point of view of the circular economy. Much research has been done on the benefits of this waste slate powder in various applications with fruitful results [24–26]. From the previous literature, the utilization of slate powder as a reinforcement in the biodegradable polymer (PLA) has yet to be used so far. Therefore, this study aims to prepare a composite based on PLA and slate powder for the 3D printer as a filament through melt extrusion with a twin screw extruder. Testing specimens are fabricated by a 3D printer using PLA-based and slate powder content (0, 5, 10, and 15 by weight) filaments. The properties of test specimens are evaluated through hardness, tensile, flexural, and impact tests. The thermo-mechanical

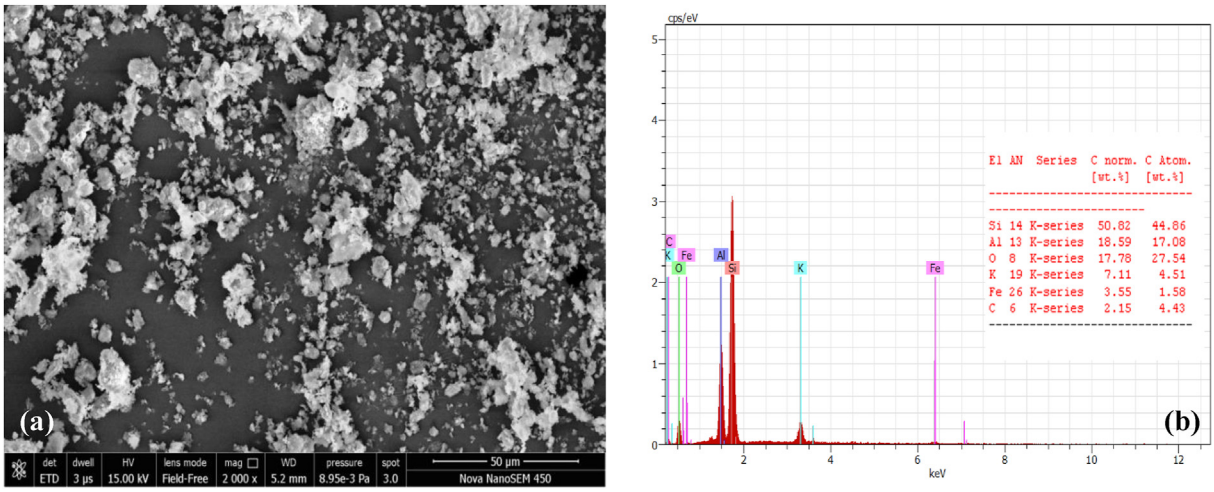

Fig. 1 – (a) Microscopic image, and (b) EDS spectrum of slate powder.

behavior of fabricated composites is examined through dynamic mechanical analysis.

2. Material and method

2.1. *Materials*

The PLA, provided by STALLION Enterprise International Trade Company Rajkot (Gujarat), India, was delivered in homopolymer pellets (density = 1.2 g/cm^3). The melting point of these pellets ranged from 120 to 130 °C, and their melt flow rate was 7 g per minute. The waste slate powder (density = 2.51 g/cm^3) was collected from the local industry, which is situated in the village of Multanpura, located in Madhya Pradesh, India. Fig. 1 depicts slate powder's microscopic picture and energy-dispersive spectroscopy (EDS) spectrum. Si, Al, K, and Fe were assigned for SiO_2, Al_2O_3, K_2O, and Fe_2O_3.

2.2. *Filament fabrication process*

3D printing filaments developed by melt extrusion using a twin screw extruder that Lab Tech Engineering Company Ltd.,

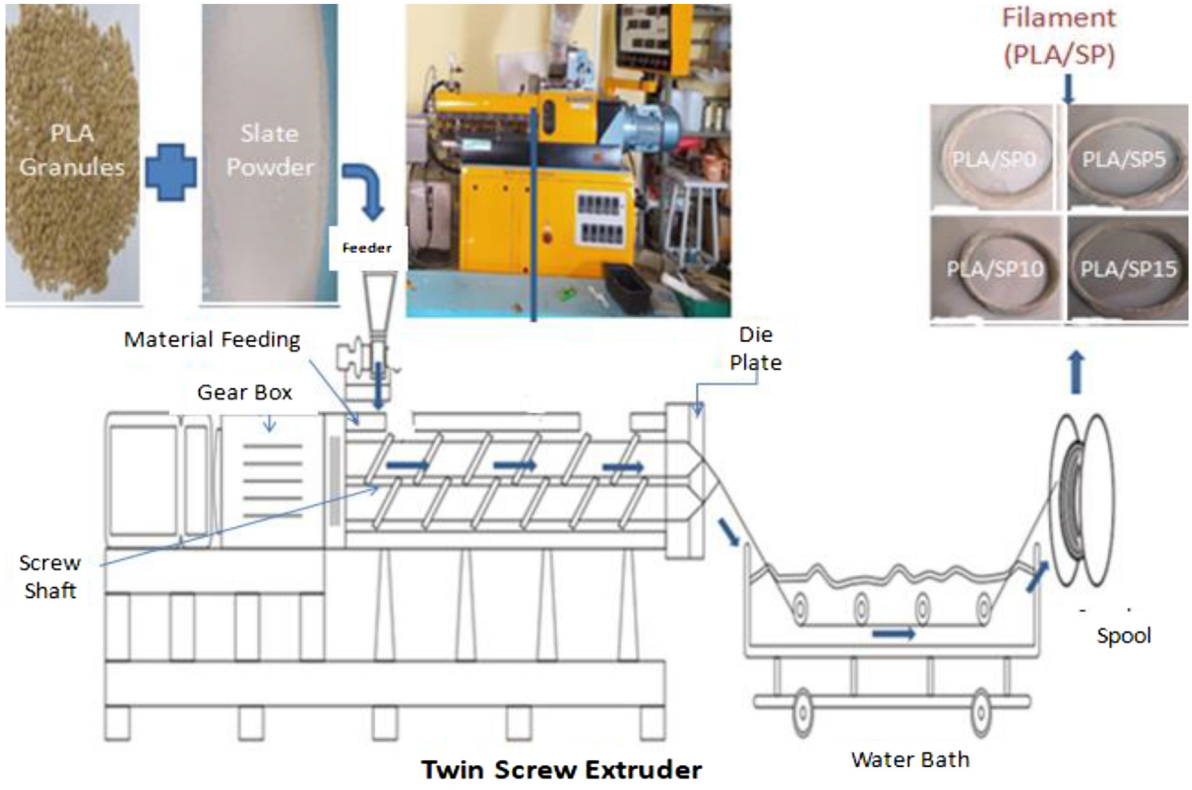

Fig. 2 – Filament fabrication process.

India, supplied. The bio-compostable PLA with slate powder was mixed in the feeder with different weight percentages from 0 to 15, in increments of 5 wt% filler content and designated as PLA/SP0 (pure PLA), PLA/SP05 (95% PLA with 5% slate powder), PLA/SP10 (90% PLA with 10% slate powder) and PLA/SP15(85% PLA with 15% slate powder). This study did not include the filler content above 15 wt% due to operational problems such as nozzle choking. Fig. 2 depicts the steps involved in the production of filament with the use of a twin screw extruder. In the extruder, there are a total of six subzones, and the length of each zone is 60 mm. The diameter of the screw is 16 mm, and the length-to-diameter ratio of the extruder is always 25. The resulting filament has a 1.75 mm diameter, the required diameter for pure PLA and PLA with slate waste composite using the 3D printer FDM machine, respectively. The temperature conditions for each zone are shown in Table 1. After departing the circular die, the filament was instantly water-cooled and wound onto a spool, as depicted in Fig. 2.

After preparing PLA/slate powder filaments, 3D printed samples are fabricated through FDM 3D printing machine (with a heated bed) manufactured by Adroitec Engineering Solutions (P) Ltd., India. The schematic diagram and pictorial view of the FDM 3D printing machine are represented in Fig. 3. To avoid the extruder blockage due to filler, a 0.4 mm nozzle was used. The process parameters of the FDM 3D printing machine during the fabrication of test samples are listed in Table 2. The specimens for different characterization as per ASTM standards are presented in Fig. 4.

3. Characterization

3.1. Mechanical properties

All the mechanical characterization is performed at ambient temperature. Tensile tests are conducted as per ASTM D638 on the servo-hydraulic universal testing machine manufactured by HEICO Pvt. Ltd. Delhi, India, in displacement mode with 2 mm/min. The flexural test is also conducted on the same machine following ASTM D790. The impact properties of fabricated PLA/SP composites are determined through the Charpy test per ASTM D6110-10. Each specimen is tested at least five times, and the results are reported using the average value. The surface hardness of fabricated composites is determined through the Shore D indenter from an average of twenty readings taken on the tensile specimen/or flexural specimen.

Table 1 – Extrusion process parameters for composite fabrication.

Process parameter	Value	Unit
Screw speed	110	rpm
Feed zone temperature	170	°C
Compression zone temperature	170	°C
Metering zone temperature	190	°C
Die temperature	180–220	°C

3.2. Dynamic mechanical analysis

Dynamic mechanical analysis (DMA) describes fabricated composites' mechanical and rheological behavior. DMA of composites evaluates the glass transition, dynamic fragility, matrix-filler interfacial compatibility, and filler effectiveness as a function of the system oscillating deformation force's temperature, time, and frequency. It is well known that high composite performance requires proper filler dispersion in the matrix material. DMA is used to assess the distribution of the different percentages of slate powder content in the PLA matrix. DMA is carried out in the tensile mode on the test specimen with the assistance of a PerkinElmer DMA 8000 in compliance with the standard specified under ASTM D4065. The experiment was carried out at temperatures ranging from 20 to 100° Celsius, with a heating rate of 2° Celsius per minute, on specimen size 40 mm × 8 mm × 4 mm, with a frequency of 1 Hz. The damping reduction (DR) value indicates the filler distribution quality inside the polymer matrix. This value is calculated using Eq. (1), in which, $(tan\,\delta)_m$ represents the damping factor of the neat PLA composite and $(tan\,\delta)_c$ indicates the damping factor of the PLA/SP composite.

$$DR(\%) = \frac{(tan\,\delta)_m - (tan\,\delta)_c}{(tan\,\delta)_m} \times 100 \quad (1)$$

4. Result and discussion

4.1. Tensile results

Fig. 5 illustrates the influence of slate powder as filler in PLA-based composite on the tensile strength, Young's modulus, and elongation at break. The outcomes reveal that the tensile strength of neat PLA composite is 30.4 ± 0.4 MPa. The tensile strength is increased by incorporating slate powder content up to 5 wt% in PLA composite. Further inclusion of filler decreases the tensile strength.

The PLA/SP composites outperformed the pure PLA sample regarding tensile modulus. With increased slate powder loading, a linear increase in the tensile modulus can be shown, improving by a relative 19% for composites with 15 wt % filler content (i.e., PLA/SP15). In the inclusion of micron-sized additives with high stiffness, like the slate powder in this instance, this behavior is ascribed to the creation of hard surfaces within the polymer matrix [23]. The elongation at break is reduced by 5.38%, 16.02%, and 20.71% with the addition of 5, 10, and 15 wt% of filler, respectively, in PLA composite. This decrease in elongation at break was predicted and attributed to the composites' enhanced stiffness due to stiffer filler with aluminosilicate content, such as slate powder. The effect of slate powder content on the typical relationship between stress-strain behavior for PLA/SP0, PLA/SP5 PLA/SP10, and PLA/SP0 composites, respectively, are shown in Fig. 6. The slate powder contents limit the mobility of PLA molecules in composites due to which the rigidity is increased, and plasticity is reduced [27]. With the incorporation of slate powder content in PLA composite, lower the elongation break as depicted in Fig. 6.

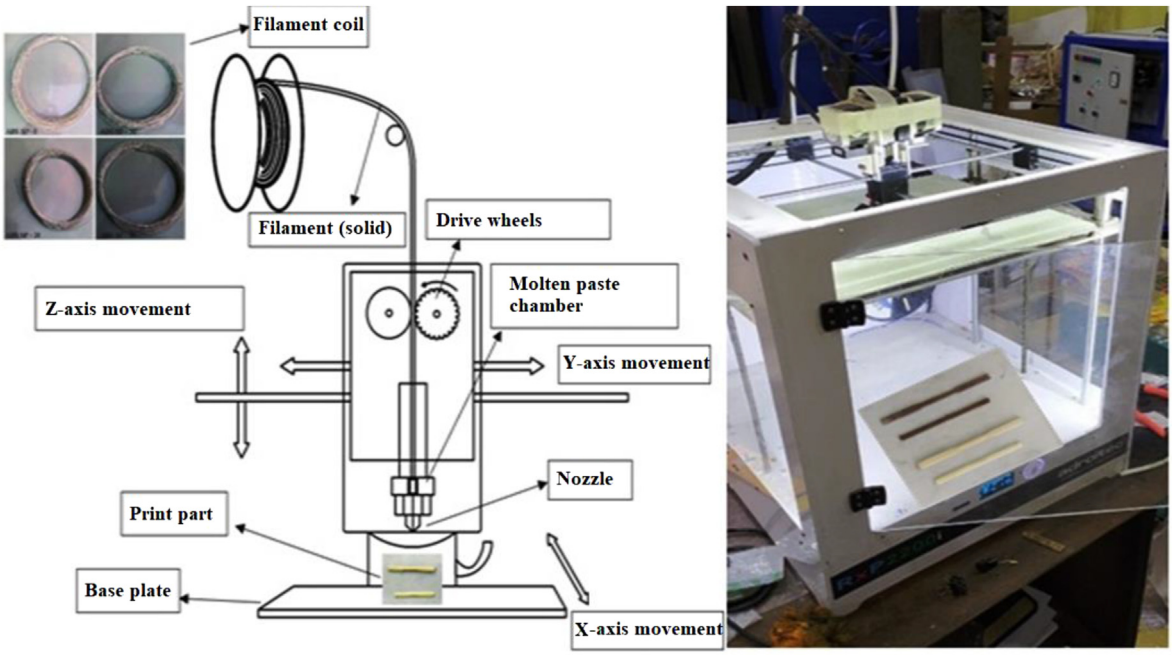

Fig. 3 – Schematic illustration of the mechanism of FDM printing.

The SEM images of the fractured surface of 3D printed tensile specimens of PLA/SP0, PLA/SP05, PLA/SP10, and PLA/SP15 composites are shown in Fig. 7. Images of 3D printed samples show the layer of filaments and void contents between the adjacent layers. The failure of material occurs due to filament breakage, filler pulls out, poor adhesion between the successive layer, and uneven melting of filament during the extrusion [28].

4.2. *Flexure properties*

A three-point bending test is used to assess the flexural characteristics of manufactured composites, and the results are presented in Fig. 8. The results show that using filler in the PLA matrix enhances flexural strength and modulus. PLA/SP0 has a flexural strength and modulus of 84.3 MPa and 3.21 GPa, which are in excellent accord with existing research [18]. The flexural strength of PLA/SP5, PLA/SP10, and PLA/SP15 composites is enhanced by 8.26%, 10.61%, and 10.02%, respectively, compared to PLA/SP0 composite. Similarly, the flexural modulus of PLA/SP5, PLA/SP10, and PLA/SP15 composites is improved by 23.67%, 29.28%, and 28.03%, respectively. The maximal flexural strength and modulus of the PLA/SP10 composite are 93.25 MPa and 4.15 GPa, respectively, for a slate powder content of 10 wt% in the PLA matrix. Integrating slate powder content in the PLA matrix above 10 wt% reduces the flexural characteristics by a marginal difference. The improvement in flexural characteristics demonstrates the inorganic filler's excellent engagement of the PLA matrix [29].

Table 2 – Process parameter of FDM 3D printing machine.

FDM operating parameter	Value
Nozzle and bed temperature	220 °C and 60 °C
Infill rate	100%
Infill pattern	Rectilinear
Raster angle	0 Degree
Layer thickness	0.1 mm
Extrusion width	0.45 mm
Printing speed	45 mm/s
Perimeter shell	3
Sample orientation	Flat

4.3. *Hardness*

Fig. 9 displays the outcomes of hardness tests conducted on the manufactured composites. With the addition of slate powder, it was discovered that the composite's hardness increased and stayed between 75 and 83 Shore D. Fig. 9 illustrates the tidy PLA's hardness value of 75 Shore D, which is in good accord with the literature [30]. With the addition of 15 wt % of slate powder, an increase of almost 11% was seen in PLA's hardness, with the highest value 83 Shore D. This rising hardness can be attributed to the presence of hard slate particles, which increase the polymer matrix's resistance to plastic deformation [31]. The PLA is a relatively stiff material that rarely exhibits plastic deformations, accounting for comparatively minor changes [32].

4.4. *Impact strength*

Fig. 9 illustrates how the amount of slate powder in the PLA matrix affects the impact strength. The impact strength of neat PLA (i.e., PLA/SP0) is 2.75 kJ/m^2, which aligns with earlier research [31]. Using slate powder in the PLA matrix increases the impact strength of manufactured composites. The impact strength value is increased by 26.18%, 30.54%, and 31.63% for 5 wt%, 10 wt%, and 15 wt% of slate powder content in PLA-based matrix composites, respectively. In Fig. 9, the 5 wt% addition of slate powder contents shows the maximum effect

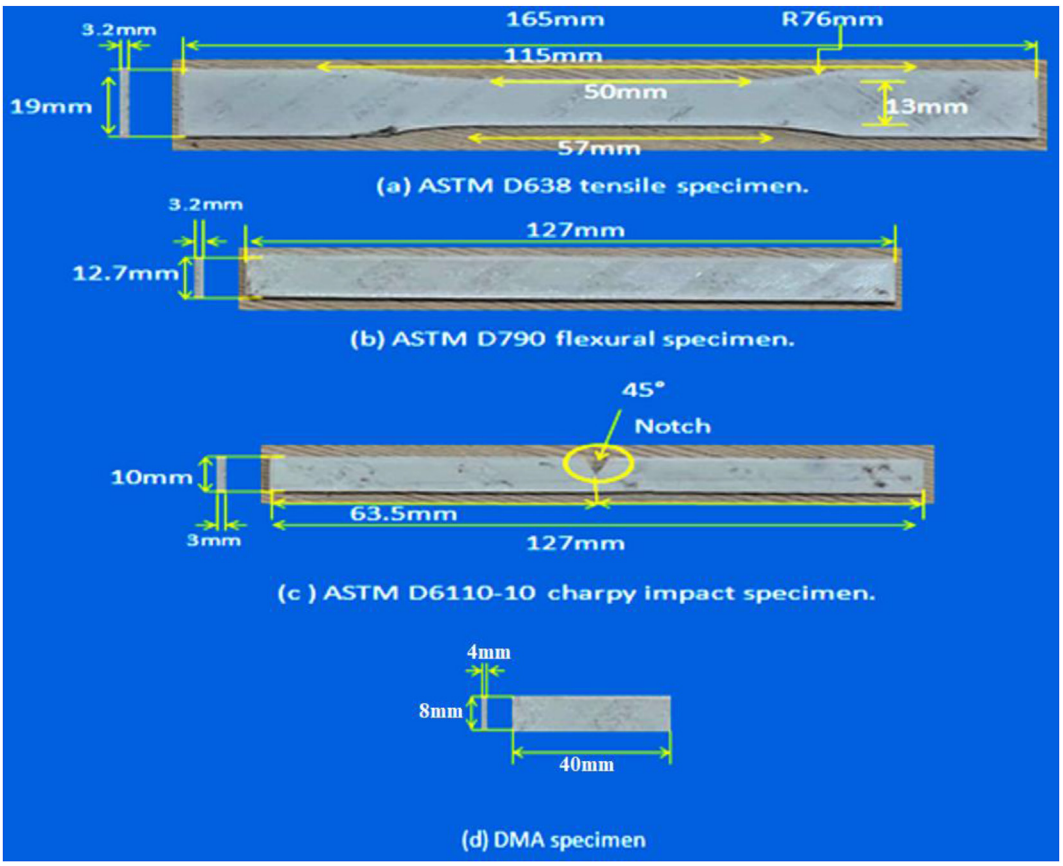

Fig. 4 – Composite specimen with dimensions.

on the impact strength value, i.e., 26.18%, further expansion from 5 wt% to 10 wt% depicts a 4.3% effect while for 10 wt% to 15 wt% reveals only 1.09% significance. This sort of improvement in the impact strength of polymeric composites is often caused by fracture deflection around the stiff filler particles and energy dissipation in the damage zone [33].

4.5. *Dynamic mechanical analysis*

Fig. 10a–c represents the effect of slate powder content in PLA-based composite on the viscoelastic behavior through storage modulus (E′), loss modulus (E″), and damping factor (tanδ) as a function of temperature. With increasing the

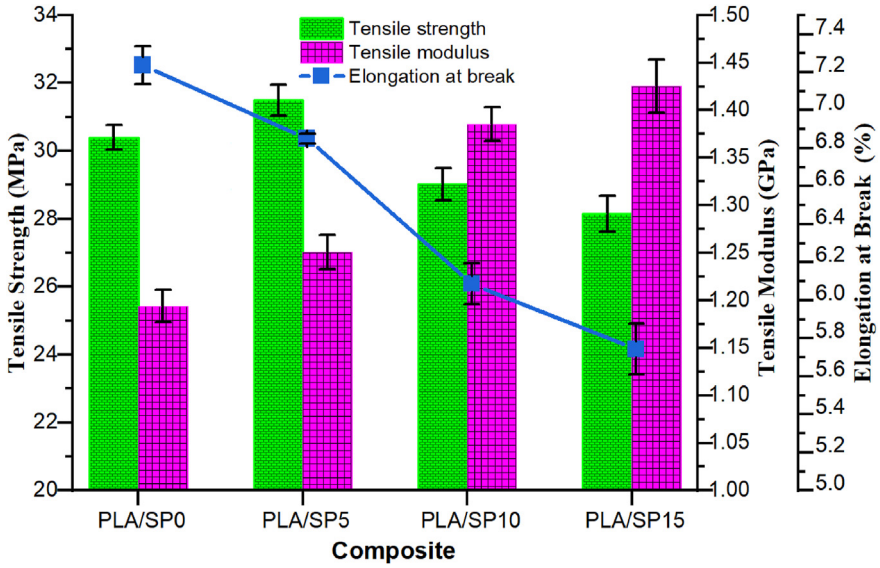

Fig. 5 – Results of tensile testing.

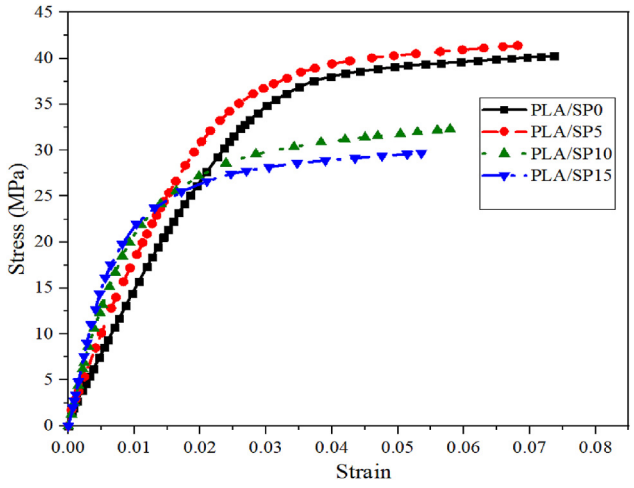

Fig. 6 – Stress-strain curves of slate powder filled PLA composites.

temperature from 20 °C to 100 °C composites' behavior is considered into three regions: glassy region (below 45 °C), glass transition region (between 50 °C and 75 °C, and rubbery region (above 80 °C) according to their molecular mobility as shown in Fig. 10a. In the glass region up to 45 °C only γ and β secondary relaxations are possible. Above 50 °C α relaxation is activated, due to which a sudden decrease in storage modulus is depicted as shown in Fig. 10a. Finally, in the rubbery region, the mobility of molecules increases; thus, the matrix polymer becomes soft from 80 °C to 100 °C [34–36]. Further, it is observed that the inclusion of slate powder in a PLA-based matrix significantly influences the viscoelastic response in the glassy region. The storage modulus of a PLA/SP0 composite (pure PLA) is 1.23 GPa at 40 °C; however, when 5, 10, and 15 wt% of slate powder are mixed to the PLA matrix, the values of E′ increase to 1.49 GPa, 1.63 GPa, and 1.67 GPa, respectively. This increment is because of the slate powder reinforcing function, which transferred the tension from the PLA to the slate powder particle. Fig. 10b represents the variation in loss modulus caused by adding the slate powder to the PLA matrix composites. The loss modulus shows the energy dissipated as heat due to molecular friction when sinusoidal deformation is applied at the same amplitude [37,38]. It is revealed that the loss modulus peak values increase with the incorporation of slate powder. The loss modulus of PLA/SP0 composite achieved a maximum value of 0.177 GPa at 48.95 °C. However, the loss modulus of PLA/SP5, PLA/SP10, and PLA/SP15 composite reached the maximum value of 0.241 GPa at 50.32 °C, 0.248 GPa at 50.33 °C and 0.26 GPa at 50.35 °C. These results reveal that slate powder content PLA composites exhibit a better capability to transfer mechanical energy as heat than the PLA/SP0 composite [39].

Fig. 10c shows the effect of slate powder content in PLA-based composite on the tan δ (damping factor) change in

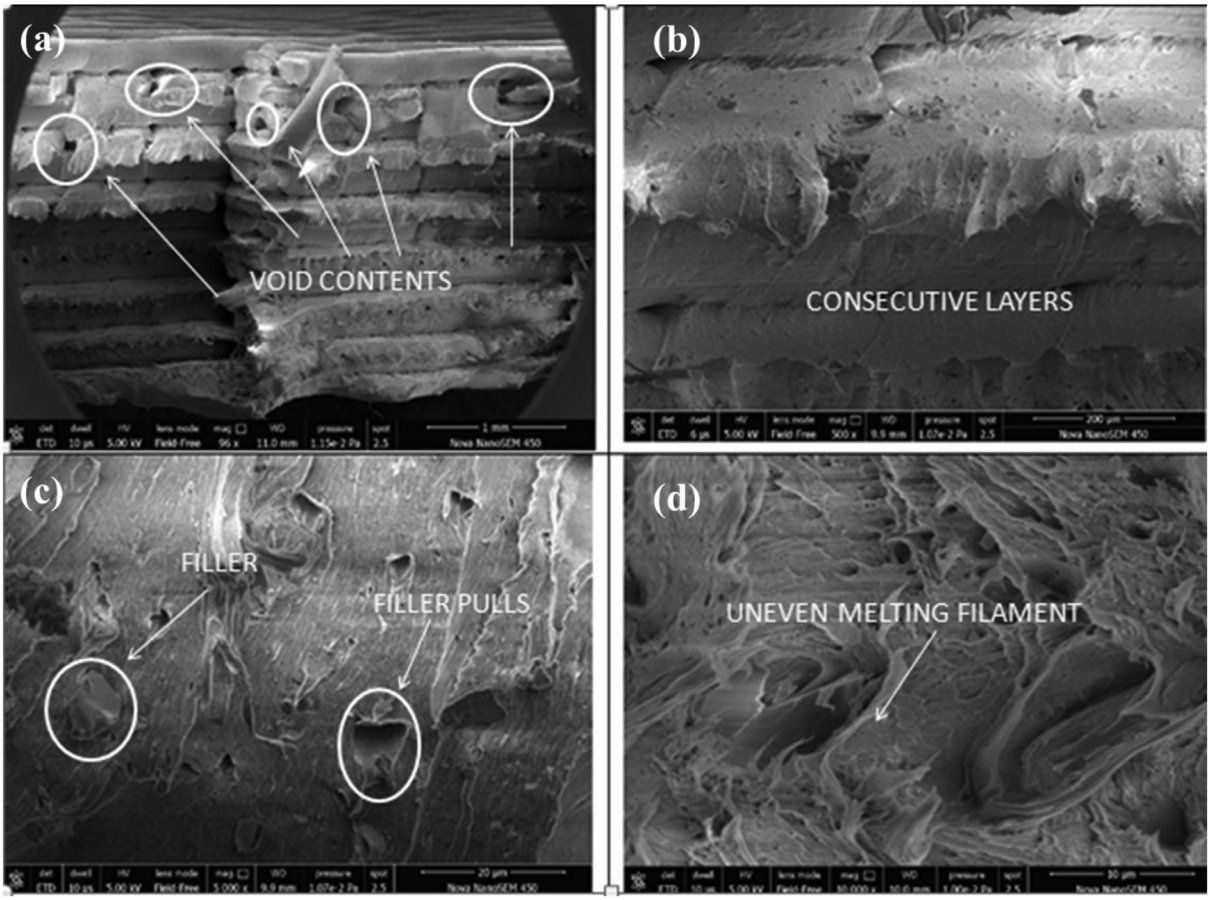

Fig. 7 – Tensile fracture zone SEM micrographs.

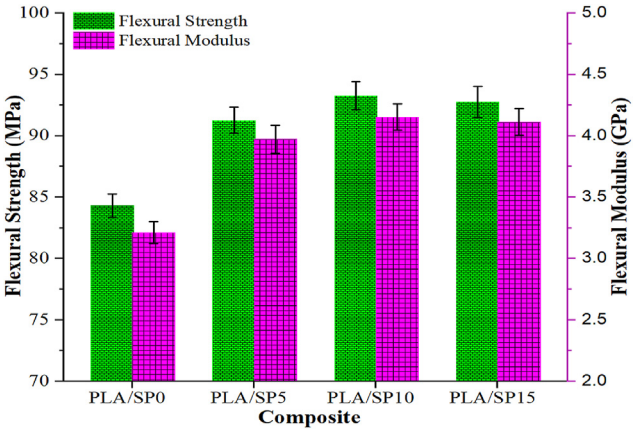

Fig. 8 – Results of flexural testing.

response to temperature. It is noticed that with the incorporation of slate powder, the glass transition temperature (T_g) of PLA/SP0 composites improved from 56.7 °C to 61.64 °C, 63.31 °C, and 64.09 °C in the case of PLA/SP5, PLA/SP10, and PLA/SP15 composites, respectively. In the glass transition region, damping characteristics represent the imperfection in the elasticity during the deformation of material energy dissipated into heat. In the case of a particulate-filled composite, molecular mobility of the polymer decreases with the addition of filler which reduces the inter-friction between molecular chains to overcome the energy dissipation. Thus, shifting of glass transition temperature to a higher temperature occurs. The damping characteristics of composites made of PLA are outlined in Table 3.

The increase in the value of damping reduction indicates a decrease in damping with the incorporation of filler [40]. This behavior of the composites shows the good compatibility of slate powder as filler with PLA matrix. Moreover, the cole-cole plot (Fig. 10d) is utilized to investigate the change in structural characteristics caused by the addition of slate powder to the PLA matrix. In this analysis, the loss modus of the composite is plotted against the storage modulus measured during the DMA testing as a function of temperature corresponding to

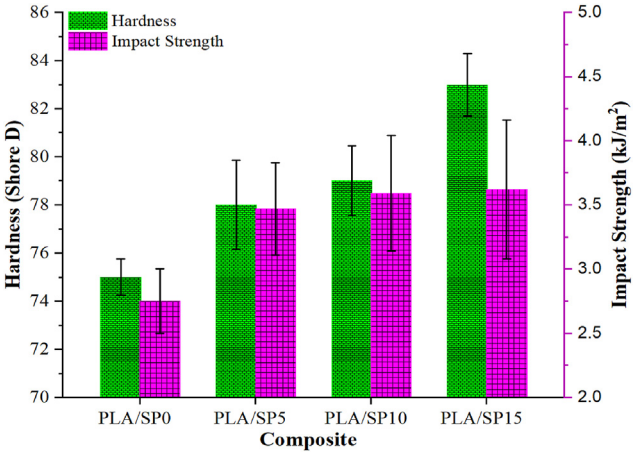

Fig. 9 – The hardness and impact strength results of the composites.

1 Hz frequency. The nature of the system can be inferred from the pattern that the cole-cole plots acquire. The semicircle shape of the cole-cole plot defines the system as homogeneous, whereas the imperfect semicircle or elliptical shape shows a heterogeneous system [37]. Fig. 10d depicts the pure PLA (PLA/SP0) composite's semicircular shape. In contrast, the addition of slate powder in the PLA matrix shows an imperfect semicircular curve due to a two-phase system, thus pointing toward good adhesion between the filler and matrix.

4.6. C- factor, entanglement density, reinforcement efficiency factor and adhesion factor

4.6.1. C- factor

The C-factor determines the effectiveness of slate powder as filler in PLA-based composite, which gives information on storage modulus with filler variation. Equation (2) is used to evaluate the value of the C-factor [41,42]:

$$C-factor = \frac{\left(E'_{gr}/E'_{rr}\right)_c}{\left(E'_{gr}/E'_{rr}\right)_m} \quad (2)$$

Where, E'_{gr} and E'_{rr} are the storage modulus values in the glassy (at 40 °C) and rubbery (at 75 °C) regions, respectively. If the value of the C-factor is high, the filler is less effective. The C-factor values obtained for different wt.% of slate powder-filled composites in PLA at the frequency of 1 Hz are depicted in Fig. 11. The PLA/SP10 composites show a minimum value of C-factor, i.e., 0.34 compared to other composites which indicate the better effectiveness (maximum stress transmit between the filler and matrix) compared to the other percentage of slate powder content in PLA composite.

4.6.2. Degree of entanglement density

It is also possible to evaluate the level of entanglement in polymer composites using dynamic mechanical analysis. The storage modulus value is utilized in Eq. (3) to calculate the entanglement degree [42]:

$$N = \frac{E'}{6RT} \quad (3)$$

Where E' represents storage modulus, R is the universal gas constant, and T denotes absolute temperature. The information regarding the modulus and toughness can be correlated with the entanglement density of polymeric composites [39,40]. Fig. 11 displays the degree of entanglement between PLA and PLA/SP composites. The entanglement density improved by up to 10 wt % of slate powder, but then it declined at higher loading. As the filler concentration increases beyond 10 wt%, the inter-particle interaction probability rises significantly, which may reduce the degree of entanglement [43]. The trend agrees with the composite's decreased flexural strength and modulus with a high slate powder dosage (~15 wt%). In contrast, impact strength, Young's, and storage modulus showed comparable results to 10 wt% slate powder-filled composites.

4.6.3. Adhesion factor

The adhesion factor (AF) is evaluated by taking the relative damping factor of the different percentages of slate powder

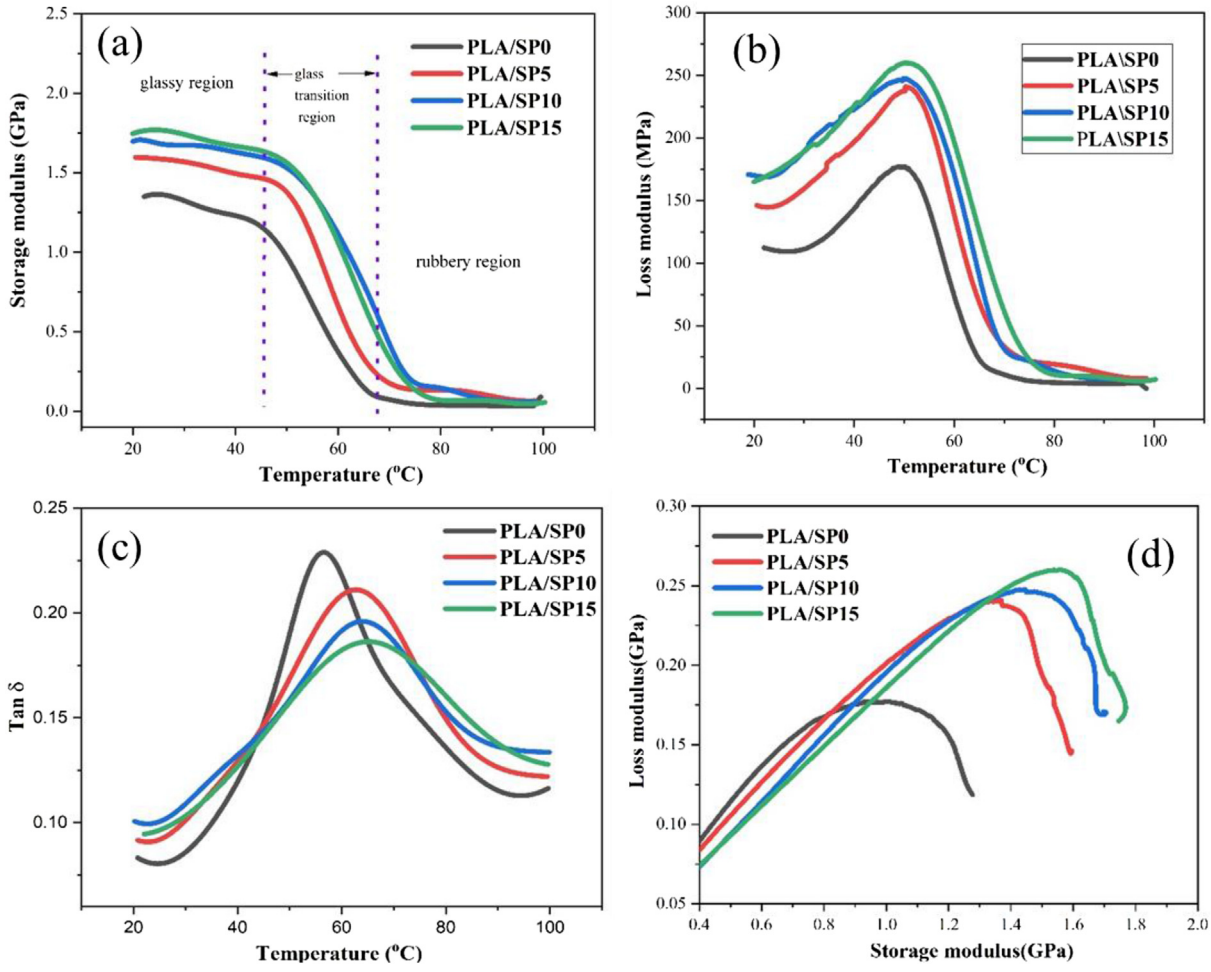

Fig. 10 – (a) Storage modulus (E′), (b) loss modulus (E″), (c) tanδ, and (d) cole-cole plot.

content-based PLA composite and pure PLA polymer as a function of the corresponding volume fraction of slate powder at a specific temperature. The AF can be defined as Eq. (4) [42]:

$$AF = \frac{1}{(1-\varnothing_f)} \frac{tan\ \delta_c}{tan\ \delta_p} - 1 \quad (4)$$

Where, $\varnothing_f$ denotes the volume fraction of filler in composite, $tan\ \delta_c$ and $tan\ \delta_p$ are damping factors for PLA/SP composite and pure PLA polymer composite, respectively. As depicted in Fig. 12, the value of the adhesion factor decreases as the degree of interaction between the slate powder and the matrix increases. The increased filler concentration reduced the damping capacity of the composites, resulting in adhesion factor reduction. A decrease in the value of the adhesion factor will occur as a direct consequence of an increase in the filler concentration, which will intensify the interaction between the slate powder particles. Similar results for the adhesion factor reduction were reported in the literature for acrylonitrile-butadiene-styrene composites [42,43].

Table 3 – Damping characteristics of the manufactured composites.

Composite	Damping factor		Damping reduction (%)
	Peak intensity	Peak temperature (°C)	
PLA/SP0	0.23	56.70	–
PLA/SP5	0.21	61.64	8.70
PLA/SP10	0.20	63.31	13.04
PLA/SP15	0.19	64.09	17.39

4.6.4. *Reinforcement efficiency factor*

The reinforcing efficiency factor provides information on filler matrix bonding by considering the impact of filler inclusion into polymeric composites. Composites' reinforcement efficiency factor can be estimated with the following equation [42]:

$$E_c = E_m(1 + rV_f) \quad (5)$$

Where E_c represents the storage modulus of slate powder-filled PLA composite while E_m denotes pure PLA composite, V_f represents the slate powder content in composite in terms of volume fraction, and r shows the reinforcing efficiency factor. Fig. 12 reveals that as the percentage of slate powder content increases in PLA-based composite, the reinforcement factor shows a downward trend. The percentage of slate powder added to the polymer composite is directly

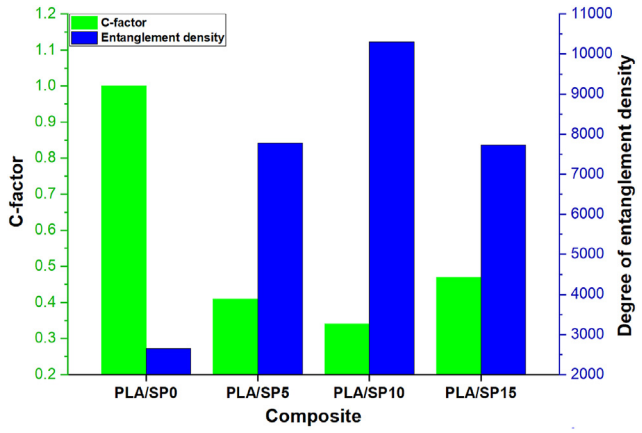

Fig. 11 – C- factor, and degree of entanglement density (mol m^{-3}).

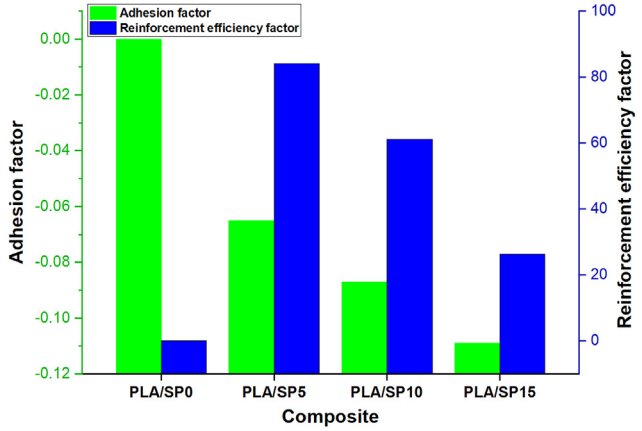

Fig. 12 – Adhesion factor and reinforcement efficiency factor.

proportional to the reinforcing factor. Because of the accurate distribution of slate powder throughout the PLA polymer, the reinforcing value of the PLA/SP5 composite is significantly higher. Increased filler concentration might result in their agglomeration, bringing structural inhomogeneities and decrement in the strength of the composites.

5. Conclusions

In the present research, the waste slate powder is utilized as filler with different weight percentages in PLA-based composite. The PLA/slate powder filaments for 3D printers are successfully fabricated with the help of a twin screw extruder. The performance of PLA/slate powder filaments is investigated through the mechanical and dynamic mechanical behavior of test specimens fabricated using a 3D printer per the ASTM standard. The outcomes of the study are summarized as follows.

- With the incorporation of slate powder content up to 5 wt %, the tensile strength of the testing specimen is improved. In contrast, the tensile modulus, hardness, and impact strength are increased by 19.03%, 10.67%, and 31.63% with 15 wt% slate powder content, respectively, in PLA-based filament.
- The flexural strength and modulus of the testing specimens are increased with slate powder content up to 10 wt% in PLA-based filaments.
- The viscoelastic response in the glassy region and the slate powder percentage in the PLA matrix show a significant effect. The storage modulus is increased by 35.77% by adding 15 wt% of slate powder content in the PLA matrix. At the same time, the increased loss modulus with slate powder content reveals composites' better ability to dissipate the mechanical energy as heat.
- The glass transition temperature of the composites is increased by 14.09% with the addition of 15 wt% of slate powder content in the PLA matrix, suggesting an increment in the thermal stability of composites.
- The minimum value of the C-factor and a higher degree of entanglement density is represented by the composite with 10 wt% slate powder content, suggesting that 10 wt% slate powder in the PLA matrix is sufficient for their effective utilization.
- The mechanical and dynamic mechanical characterization shows significant insight into using waste slate powder as filler in PLA matrix as a mechanically robust material for 3D printer filaments.

Declaration of competing interest

The authors declare that they have no known competing financial interests or personal relationships that could have appeared to influence the work reported in this paper.

REFERENCES

[1] Srivastava M, Rathee S, Patel V, Kumar A, Koppad PG. A review of various materials for additive manufacturing: recent trends and processing issues. J Mater Res Technol 2022;21:2612–41.
[2] Alarifi IM. Mechanical properties and numerical simulation of FDM 3D printed PETG/carbon composite unit structures. J Mater Res Technol 2023;23:656–69.
[3] Jagadeesh P, Puttegowda M, Rangappa SM, Alexey K, Gorbatyuk S, Khan A, Doddamani M, Siengchin S. A comprehensive review on 3D printing advancements in polymer composites: technologies, materials, and applications. Int J Adv Manuf Technol 2022;121:127–69.
[4] Fekete I, Ronkay F, Lendvai L. Highly toughened blends of poly(lactic acid) (PLA) and natural rubber (NR) for FDM-based 3D printing applications: the effect of composition and infill pattern. Polym Test 2021;99:107205.
[5] Kumar S, Ramesh MR, Doddamani M, Rangappa SM, Siengchin S. Mechanical characterization of 3D printed MWCNTs/HDPE nanocomposites. Polym Test 2022;114:107703.

[6] Liu Z, Lei Q, Xing S. Mechanical characteristics of wood, ceramic, metal and carbon fiber-based PLA composites fabricated by FDM. J Mater Res Technol 2019;8:3741–51.
[7] Rajeshkumar G, Seshadri SA, Devnani GL, Sanjay MR, Siengchin S, Maran JP, Al-Dhabi NA, Karuppiah P, Mariadhas VA, Sivarajasekar N, Anuf AR. Environment friendly, renewable and sustainable poly lactic acid (PLA) based natural fiber reinforced composites-A comprehensive review. J Clean Prod 2021;310:127483.
[8] Lendvai L, Patnaik A. The effect of coupling agent on the mechanical properties of injection molded polypropylene/wheat straw composites. Acta Technica Jaurinensis 2022;15:232–8.
[9] Lendvai L, Brenn D. Mechanical, morphological and thermal characterization of compatibilized poly(lactic acid)/thermoplastic starch blends. Acta Technica Jaurinensis 2020;13:1–13.
[10] Qian S, Mao H, Sheng K, Lu J, Luo Y, Hou C. Effect of low-concentration alkali solution pretreatment on the properties of bamboo particles reinforced poly(lactic acid) composites. J Appl Polym Sci 2013;130:1667–74.
[11] Praveenkumara J, Madhu P, Gowda TGY, Sanjay MR, Siengchin S. A comprehensive review on the effect of synthetic filler materials on fiber-reinforced hybrid polymer composites. J Textil Inst 2022;113:1231–9.
[12] Jagadeesh P, Puttegowda M, Mavinkere RS, Siengchin S. Influence of nanofillers on biodegradable composites: a comprehensive review. Polym Compos 2021;42:5691–711.
[13] Jagadeesh P, Puttegowda M, Thyavihalli GYG, Rangappa SM, Siengchin S. Effect of natural filler materials on fiber reinforced hybrid polymer composites: an Overview. J Nat Fibers 2022;19:4132–47.
[14] Prashantha K, Roger F. Multifunctional properties of 3D printed poly(lactic acid)/graphene nanocomposites by fused deposition modeling. J Macromol Sci, Pure Appl Chem 2017;54:24–9.
[15] Guo R, Ren Z, Bi H, Song Y, Xu M. Effect of toughening agents on the properties of poplar wood flour/poly (lactic acid) composites fabricated with fused deposition modeling. Eur Polym J 2018;107:34–45.
[16] Ambone T, Joseph S, Deenadayalan E, Mishra S, Jaisankar S, Saravanan P. Polylactic acid (pla) biocomposites filled with waste leather buff (WLB). J Polym Environ 2017;25:1099–109.
[17] Hamdan MHM, Siregar JP, Rejab MRM, Bachtiar D, Jamiluddin J, Tezara C. Effect of maleated anhydride on mechanical properties of rice husk filler reinforced pla matrix polymer composite. International Journal of Precision Engineering and Manufacturing - Green Technology 2019;6:113–24.
[18] Nagarjun J, Kanchana J, RajeshKumar G, Manimaran S, Krishnaprakash M. Enhancement of mechanical behavior of PLA matrix using tamarind and date seed micro fillers. J Nat Fibers 2022;19:4662–74.
[19] Clarizio SC, Tatara RA. Tensile strength, elongation, hardness, and tensile and flexural moduli of PLA filled with glycerol-plasticized DDGS. J Polym Environ 2012;20:638–46.
[20] Koutsomitopoulou AF, Bénézet JC, Bergeret A, Papanicolaou GC. Preparation and characterization of olive pit powder as a filler to PLA-matrix bio-composites. Powder Technol 2014;255:10–6.
[21] Altun M, Celebi M, Ovali S. Preparation of the pistachio shell reinforced PLA biocomposites: effect of filler treatment and PLA maleation. J Thermoplast Compos Mater 2022;35:1342–57.
[22] Yang L, Li S, Zhou X, Liu J, Li Y, Yang M, Yuan Q, Zhang W. Effects of carbon nanotube on the thermal, mechanical, and electrical properties of PLA/CNT printed parts in the FDM process. Synth Met 2019;253:122–30.
[23] Zhang L, Chai W, Li W, Semple K, Yin N, Zhang W, Dai C. Intumescent-grafted bamboo charcoal: a natural nontoxic fire-retardant filler for polylactic acid (PLA) composites. ACS Omega 2021;6:26990–7006.
[24] Samper MD, Petrucci R, Sánchez-Nacher L, Balart R, Kenny JM. New environmentally friendly composite laminates with epoxidized linseed oil (ELO) and slate fiber fabrics. Compos B Eng 2015;71:203–9.
[25] Carbonell-Verdú A, García-García D, Jordá A, Samper MD, Balart R. Development of slate fiber reinforced high density polyethylene composites for injection molding. Compos B Eng 2015;69:460–6.
[26] Binda FF, Oliveira VA, Fortulan CA, Palhares LB, Santos CG. Friction elements based on phenolic resin and slate powder. J Mater Res Technol 2020;9:3378–83.
[27] Ho M, Lau K, Wang H, Hui D. Improvement on the properties of polylactic acid (PLA) using bamboo charcoal particles. Compos B Eng 2015;81:14–25.
[28] Lay M, Thajudin NLN, Hamid ZAA, Rusli A, Abdullah MK, Shuib RK. Comparison of physical and mechanical properties of PLA, ABS and nylon 6 fabricated using fused deposition modeling and injection molding. Compos B Eng 2019;176:107341.
[29] Lendvai L, Singh T, Fekete G, Patnaik A, Dogossy G. Utilization of waste marble dust in poly(lactic acid)-based biocomposites: mechanical, thermal and wear properties. J Polym Environ 2021;29:2952–63.
[30] Teymoorzadeh H, Rodrigue D. Biocomposites of wood flour and polylactic acid: processing and properties. J Biobased Mater Bioenergy 2015;9:252–7.
[31] Ramachandran MG, Rajeswari N. Influence of nano silica on mechanical and tribological properties of additive manufactured PLA bio nanocomposite. Silicon 2022;14:703–9.
[32] Rimpongpisarn T, Wattanathana W, Sukthavorn K, Nootsuwan N, Hanlumyuang Y, Veranitisagul C, Laobuthee A. Novel luminescent PLA/$MgAl_2O_4$:Sm^{3+} composite filaments for 3D printing application. Mater Lett 2019;237:270–3.
[33] Fu S-Y, Feng X-Q, Lauke B, Mai Y-W. Effects of particle size, particle/matrix interface adhesion and particle loading on mechanical properties of particulate-polymer composites. 2008 Compos B Eng 2008;39:933–61.
[34] Rahman MM, Zainuddin S, Hosur MV, Malone JE, Salam MBA, Kumar A, Jeelani S. Improvements in mechanical and thermo-mechanical properties of e-glass/epoxy composites using amino functionalized MWCNTs. Compos Struct 2012;94:2397–406.
[35] Kumar V, Dev A, Gupta AP. Studies of poly(lactic acid) based calcium carbonate nanocomposites. Compos B Eng 2014;56:184–8.
[36] Huda MS, Drzal LT, Mohanty AK, Misra M. Chopped glass and recycled newspaper as reinforcement fibers in injection molded poly(lactic acid) (PLA) composites: a comparative study. Compos Sci Technol 2006;66:1813–24.
[37] Choudhary M, Singh T, Dwivedi M, Patnaik A. Waste marble dust-filled glass fiber-reinforced polymer composite Part I: physical, thermomechanical, and erosive wear properties. Polym Compos 2019;40:4113–24.
[38] Choudhary M, Sharma A, Dwivedi M, Patnaik A. A Comparative study of the physical, mechanical and thermo-mechanical behavior of GFRP composite based on fabrication techniques. Fibers Polym 2019;20:823–31.

[39] Yuzay IE, Auras R, Selke S. Poly(lactic acid) and zeolite composites prepared by melt processing: morphological and physical-mechanical properties. J Appl Polym Sci 2010;115:2262–70.
[40] Bleach NC, Nazhat SN, Tanner KE, Kellom M, Aki PT, Orm A. Effect of filler content on mechanical and dynamic mechanical properties of particulate biphasic calcium phosphatepolylactide composites. Biomaterials 2002;23:1579–85.
[41] Gregorova A, MacHovsky M, Wimmer R. Viscoelastic properties of mineral-filled poly(lactic acid) composites. International Journal of Polymer Science 2012;2012:252981.
[42] Jyoti J, Singh BP, Arya AK, Dhakate SR. Dynamic mechanical properties of multiwall carbon nanotube reinforced ABS composites and their correlation with entanglement density, adhesion, reinforcement and C factor. RSC Adv 2016;6:3997–4006.
[43] Pande AK, Kumar R, Kachhavah VS, Kar KK. Mechanical and thermal behaviours of graphite flake reinforced acrylonitrile butadiene styrene composites and their correlation with entanglement density, adhesion, reinforcement and C factor. RSC Adv 2016;6:50559–71.